

Viable scalar spectral tilt and tensor-to-scalar ratio in near-matter bounces

Rathul Nath Raveendran[†] and L. Sriramkumar[‡]

[†]*The Institute of Mathematical Sciences, HBNI, CIT Campus, Chennai 600113, India*

[‡]*Department of Physics, Indian Institute of Technology Madras, Chennai 600036, India*

In a recent work, we had constructed a model consisting of two fields—a canonical scalar field and a non-canonical ghost field—that had sourced a symmetric matter bounce scenario. The model had involved only one parameter, *viz.* the scale associated with the bounce. For a suitable value of the parameter, the model had led to strictly scale invariant power spectra with a COBE normalized scalar amplitude and a rather small tensor-to-scalar ratio. In this work, we extend the model to achieve near-matter bounces, which contain a second parameter apart from the bounce scale. As the new model does not seem to permit analytical evaluation of the scalar modes near the bounce, with the aid of techniques which we had used in our earlier work, we compute the scalar and the tensor power spectra *numerically*. For appropriate values of the additional parameter, we find that the model produces red spectra with a scalar spectral tilt and a small tensor-to-scalar ratio which are consistent with the recent observations of the anisotropies in the cosmic microwave background by Planck.

I. INTRODUCTION

The inflationary scenario is the most popular paradigm to describe the origin of the perturbations in the early universe [1–9]. Despite the fact that the recent observations of the Cosmic Microwave Background (CMB) anisotropies by Planck has led to unprecedented constraints on the inflationary parameters [10, 11], there exist many models of inflation that remain consistent with the data [12–15], even giving rise to the concern if inflation can be falsified at all [16]. In such a situation, it seems imperative to systematically explore alternatives to inflation.

Classical bouncing scenarios provide an alternative to the inflationary paradigm for the creation of the primordial perturbations [17–23]. In these scenarios, the universe undergoes a period of contraction before it begins to expand and, under certain conditions, it is possible to impose well motivated initial conditions during the contracting phase in a manner akin to inflation. The shape of the primordial spectra generated in such scenarios is largely determined by the form of the contraction during the early stages. For instance, the so-called matter bounces are known to generate scale invariant spectra, as they are ‘dual’ to de Sitter inflation [24, 25]. Due to this reason, near-matter bounces can be expected to lead to nearly scale invariant primordial spectra, as is required by the CMB observations.

While it is rather easy to build inflationary models that are consistent with the observations, it proves to be quite involved to construct viable bouncing models. The difficulties largely arise due to the fact that the null energy condition has to be violated near the bounce, which leads to certain pathologies at the level of the background as well as the perturbations (for a discussion on the various issues one encounters, see, for example, the introductory section of Ref. [26]). The simplest of the bouncing models are those whose scale factors are symmetric about the bounce. However, it has been found that such models can lead to a large tensor-to-scalar ratio beyond the current

constraints [27]. Recently, we had constructed a model consisting of a canonical and a non-canonical (as well as ghost) field to drive a symmetric matter bounce [26]. We had shown (both analytically and numerically) that the model leads to strictly scale invariant primordial spectra and a viable tensor-to-scalar ratio as well as insignificant isocurvature perturbations. We had found that the amplitude of the scalar perturbations are considerably enhanced during the null energy condition violating phase resulting in a small tensor-to-scalar ratio after the bounce. In this work, we extend our earlier model so that it also leads to a scalar spectral tilt that is consistent with the observations.

This paper is organized as follows. In the following section, we shall describe the scale factor of our interest and the sources that can drive such a background. In Sec. III, we shall discuss the simpler case of the evolution of the tensor perturbations and evaluate the tensor power spectra prior to the bounce. In Sec. IV, we shall arrive at the equations governing the scalar perturbations. In Sec. V, we shall solve the equations governing the scalar and tensor perturbations numerically to determine their evolution across the bounce. We shall also present the essential results, *viz.* the scalar and tensor power spectra (evaluated after the bounce) that we obtain in the model. In Sec. VI, we shall conclude with a brief summary.

Let us now make a few clarifying remarks on our conventions and notations. We shall adopt natural units such that $\hbar = c = 1$, and set the Planck mass to be $M_{\text{Pl}} = (8\pi G)^{-1/2}$. We shall work with the metric signature of $(-, +, +, +)$. Note that the Greek indices shall denote the spacetime coordinates, whereas the Latin indices shall represent the spatial coordinates, except for k which we shall reserve for denoting the wavenumber. Also, as usual, an overdot and an overprime shall denote differentiation with respect to the cosmic and the conformal time coordinates, respectively. Moreover, we shall also work with a new time variable that we have introduced in an earlier work on bouncing scenarios, *viz.* e-N-folds, which we shall denote as \mathcal{N} [28, 29].

II. BACKGROUND AND SOURCES

In this section, we shall construct sources involving two scalar fields to drive near-matter bounces. We shall consider the background to be the spatially flat, Friedmann-Lemaître-Robertson-Walker (FLRW) metric that is described by the line element

$$\begin{aligned} ds^2 &= -dt^2 + a^2(t) \delta_{ij} dx^i dx^j \\ &= a^2(\eta) (-d\eta^2 + \delta_{ij} dx^i dx^j), \end{aligned} \quad (1)$$

where $a(t)$ is the scale factor and $\eta = \int dt/a(t)$ denotes the conformal time coordinate. We shall assume that the scale factor describing the bounce is given in terms of the conformal time as follows:

$$a(\eta) = a_0 (1 + k_0^2 \eta^2)^{1+\lambda} = a_0 \left(1 + \frac{\eta^2}{\eta_0^2}\right)^{1+\lambda}, \quad (2)$$

where a_0 is the value of the scale factor at the bounce (*i.e.* at $\eta = 0$), $k_0 = 1/\eta_0$ is the scale associated with the bounce¹, while $\lambda \geq 0$. Note that $\lambda = 0$ corresponds to the specific case of matter bounce we had considered in our earlier work [26]. As we shall see later, a non-zero but small λ (such that $0 < \lambda \ll 1$) leads to a scalar spectral tilt suggested by the CMB observations.

We find that the Hubble parameter associated with the scale factor (2) can be expressed as

$$H^2 = \left[\frac{2k_0(1+\lambda)}{a_0}\right]^2 \left[\frac{1}{(a/a_0)^\gamma} - \frac{1}{(a/a_0)^\delta}\right], \quad (3)$$

where $\gamma = (3 + 2\lambda)/(1 + \lambda)$ and $\delta = 2(2 + \lambda)/(1 + \lambda)$. Recall that, according to the first Friedmann equation, $H^2 = \rho/(3M_{\text{Pl}}^2)$, with ρ being the total energy density of the sources driving the background. Therefore, the right hand side of the expression (3) suggests that the scale factor (2) can be driven by two sources described by the equations of state $w_1 = -\lambda/[3(1 + \lambda)]$ and $w_2 = (1 - \lambda)/[3(1 + \lambda)]$. Moreover, the second source has to have negative energy density, a property which ensures that the Hubble parameter vanishes at the bounce (*i.e.* when $a = a_0$). Before we proceed further to model the two sources in terms of scalar fields, a couple of points require clarification to ally possible concerns related to the fact that we are working with a spatially flat FLRW universe. Note that, if a non-zero spatial curvature is present, at very early times, the corresponding contribution to the first Friedmann equation (3) (which behaves as a^{-2}) can dominate the dynamics of the background. However, at later times during the contracting phase, these effects will quickly become sub-dominant and the

dynamics will be essentially governed by the first source (whose energy density behaves as a^{-3}) we have described above. More importantly, in our discussion below, we shall assume that the perturbations originated during the phase wherein the spatial curvature is sub-dominant. Further, it can be shown that the presence of spatial curvature does not affect the evolution of the perturbations around the bounce (in this context, see Ref. [30]). Due to these reasons, we believe that it is consistent to work with a spatially flat FLRW universe.

The two sources discussed above can be modeled in terms of two scalar fields—a canonical scalar field, say, ϕ , characterized by the potential $V(\phi)$ and a non-canonical ghost field, say, χ —that are described by the action

$$S[\phi, \chi] = - \int d^4x \sqrt{-g} \left[-X^{\phi\phi} + V(\phi) + U_0 \left(X^{\chi\chi}\right)^b \right] \quad (4)$$

with U_0 and b being positive constants. The quantities $X^{\phi\phi}$ and $X^{\chi\chi}$ are the kinetic terms defined as

$$X^{\phi\phi} = -\frac{1}{2} \partial_\mu \phi \partial^\mu \phi, \quad (5a)$$

$$X^{\chi\chi} = -\frac{1}{2} \partial_\mu \chi \partial^\mu \chi. \quad (5b)$$

The stress-energy tensor associated with these fields can be obtained to be

$$T_{\nu(\phi)}^\mu = \partial^\mu \phi \partial_\nu \phi - \delta_\nu^\mu \left[-X^{\phi\phi} + V(\phi) \right], \quad (6a)$$

$$T_{\nu(\chi)}^\mu = -b U_0 \left(X^{\chi\chi}\right)^{b-1} \partial^\mu \chi \partial_\nu \chi - \delta_\nu^\mu U_0 \left(X^{\chi\chi}\right)^b. \quad (6b)$$

It should be evident that we have invoked the ghost field χ in order to achieve the violation of the null energy condition around the bounce. While this is the simplest method possible, ghost fields are considered to be undesirable because of the fact that they do not permit a stable quantum vacuum. In this work, our primary aim will be to study the evolution of the curvature and isocurvature perturbations across the bounce. As we shall see, we are able to circumvent challenges that arise (due to the presence of the ghost field) in the evolution of these perturbations through the bounce.

Let us first consider the behavior of the ghost field χ . For a homogeneous field, it is straightforward to show that

$$T_{0(\chi)}^0 = -\rho_\chi = (2b - 1) U_0 \left(X^{\chi\chi}\right)^b, \quad (7a)$$

$$T_{j(\chi)}^i = p_\chi \delta_j^i = -U_0 \left(X^{\chi\chi}\right)^b \delta_j^i, \quad (7b)$$

where, evidently, ρ_χ and p_χ are the energy density and pressure associated with the χ field. Note that ρ_χ is negative for $b > 1/2$ and $p_\chi = \rho_\chi/(2b - 1)$, corresponding to $w_\chi = p_\chi/\rho_\chi = 1/(2b - 1)$. If we set $w_\chi = w_2 = (1 - \lambda)/[3(1 + \lambda)]$, which corresponds to $b = (2 + \lambda)/(1 - \lambda)$,

¹ To be precise, the energy scale associated with the bounce is actually given by k_0/a_0 . For instance, the amplitudes of the scalar and tensor power spectra are determined *only* by this combination (in this context, see the discussion in Ref. [26]).

then the energy density of the field χ can be expressed as

$$\rho_\chi = -3 M_{\text{Pl}}^2 \left[\frac{2 k_0 (1 + \lambda)}{a_0} \right]^2 \frac{1}{(a/a_0)^\delta}. \quad (8)$$

In this expression for ρ_χ , we have chosen the overall constant such that it corresponds to the second term in the expression (3) for H^2 through the first Friedmann equation.

Let us now turn to the behavior of the canonical scalar field ϕ . The non-zero components of the stress-energy tensor associated with the homogeneous field ϕ are given by

$$T_{0(\phi)}^0 = -\rho_\phi = -\frac{\dot{\phi}^2}{2} - V(\phi), \quad (9a)$$

$$T_{j(\phi)}^i = p_\phi \delta_j^i = \left[\frac{\dot{\phi}^2}{2} - V(\phi) \right] \delta_j^i. \quad (9b)$$

In order to lead to the first term in the expression (3) for H^2 (through the first Friedmann equation), we require ρ_ϕ to behave as

$$\rho_\phi = 3 M_{\text{Pl}}^2 \left[\frac{2 k_0 (1 + \lambda)}{a_0} \right]^2 \frac{1}{(a/a_0)^\gamma}, \quad (10)$$

which implies that $w_\phi = p_\phi/\rho_\phi = w_1 = -\lambda/[3(1+\lambda)]$. These results and Eqs. (9) lead to

$$\dot{\phi}^2 = 2 \left(\frac{3 + 2\lambda}{3 + 4\lambda} \right) V(\phi). \quad (11)$$

Using Eqs. (9a), (10), (11) and the scale factor (2), it is straightforward to show that the evolution of the field ϕ can be expressed in terms of the scale factor $a(\eta)$ as

$$\phi(a) - \phi_0 = 2 \sqrt{(1 + \lambda)(3 + 2\lambda)} M_{\text{Pl}} \times \cosh^{-1} \left\{ [a(\eta)/a_0]^{1/[2(1+\lambda)]} \right\}, \quad (12)$$

where ϕ_0 is the value of ϕ at the bounce, *i.e.* when $a = a_0$. From the above expression for $\phi(a)$ and Eq. (11), the corresponding potential $V(\phi)$ can be obtained to be

$$V(\phi) = 2(3 + 4\lambda)(1 + \lambda) \left(\frac{M_{\text{Pl}} k_0}{a_0} \right)^2 \times \cosh^{-2(3+2\lambda)} \left[\frac{(\phi - \phi_0)/M_{\text{Pl}}}{2 \sqrt{(1 + \lambda)(3 + 2\lambda)}} \right]. \quad (13)$$

Two points need to be stressed regarding the model we have constructed. Firstly, note that the potential $V(\phi)$ above as well as the complete system involving the two scalar fields ϕ and χ described by the action (4) depend only on the two parameters k_0/a_0 and λ , as ϕ_0 and U_0 do not play any non-trivial role in the dynamics. Secondly, when $\lambda = 0$, the action reduces to the model that leads to the matter bounce scenario that we have considered earlier [26].

III. THE TENSOR MODES AND THE RESULTING POWER SPECTRUM

The tensor perturbations are always simpler to study because the equations governing their evolution depends only on the scale factor that describes the FLRW universe and not on the nature of the source that drives the background. In this section, we shall discuss the tensor power spectrum arising in the near-matter bounces of our interest. As the scale factor (2) reduces to a power law form at early times, *i.e.* when $\eta \ll -\eta_0$, the modes and power spectrum well before the bounce are straightforward to arrive at. In a later section, we shall numerically evolve the tensor perturbations across the bounce and evaluate the power spectrum *after* the bounce. We shall see that, while the bounce alters the amplitude of the tensor power spectrum, it does not change its shape.

Let us quickly summarize a few essential points concerning the tensor perturbations. If the tensor perturbations are characterized by γ_{ij} , then the spatially flat FLRW metric containing the perturbations can be expressed as [31]

$$ds^2 = a^2(\eta) \left\{ -d\eta^2 + [\delta_{ij} + \gamma_{ij}(\eta, \mathbf{x})] d\mathbf{x}^i d\mathbf{x}^j \right\}. \quad (14)$$

The Fourier modes h_k corresponding to the tensor perturbations are governed by the differential equation

$$h_k'' + 2 \frac{a'}{a} h_k' + k^2 h_k = 0 \quad (15)$$

and, if we write $h_k = (\sqrt{2}/M_{\text{Pl}}) u_k/a$, then the Mukhanov-Sasaki variable u_k satisfies the differential equation

$$u_k'' + \left(k^2 - \frac{a''}{a} \right) u_k = 0. \quad (16)$$

The tensor power spectrum evaluated at a specific time is defined as

$$\mathcal{P}_T(k) = 4 \frac{k^3}{2\pi^2} |h_k(\eta)|^2 \quad (17)$$

and the corresponding tensor spectral index n_T is given by

$$n_T = \frac{d \ln \mathcal{P}_T(k)}{d \ln k}. \quad (18)$$

During the early contracting phase, *i.e.* when $\eta \ll -\eta_0$, the scale factor (2) behaves as $a(\eta) \propto \eta^{2(1+\lambda)}$. Due to this reason, the equation (16) describing the Mukhanov-Sasaki variable u_k reduces to

$$u_k'' + \left[k^2 - \frac{2(1 + \lambda)(1 + 2\lambda)}{\eta^2} \right] u_k \simeq 0. \quad (19)$$

For modes of cosmological interest, we can impose the standard Bunch-Davies initial conditions at early times when $k\eta \ll -[2(1 + \lambda)(1 + 2\lambda)]^{1/2}$. In such a case,

the solution to above equation which satisfies the Bunch-Davies initial condition is found to be

$$u_k(\eta) \simeq \left(\frac{-\pi k \eta}{4} \right)^{1/2} e^{i(\nu+1/2)\pi/2} H_\nu^{(1)}(-k\eta), \quad (20)$$

where $H_\nu^{(1)}(x)$ denotes Hankel function of the first kind, while $\nu = 3/2 + 2\lambda$. The tensor power spectrum evalu-

ated as one approaches the bounce can be expressed as

$$\mathcal{P}_T(k) = \frac{1}{2\pi^2 M_{\text{Pl}}^2} \left| \frac{\Gamma(\nu)}{\Gamma(3/2)} \right|^2 \left[\frac{k}{a(\eta)} \right]^2 \left(\frac{-k\eta}{2} \right)^{1-2\nu}. \quad (21)$$

The corresponding spectral index n_T is evidently given by

$$n_T = -4\lambda, \quad (22)$$

which clearly reduces to zero when $\lambda = 0$ corresponding to the case of the matter bounce. We shall later evolve the tensor perturbations numerically and compute the power spectra before as well as after the bounce. We shall find that the above analytical spectrum matches the numerical results prior to the bounce and the spectral shape is retained as the modes are evolved across the bounce.

IV. ARRIVING AT THE EQUATIONS GOVERNING THE SCALAR PERTURBATIONS

Since we are working with two scalar fields, as is well known, there will arise two *independent* scalar degrees of freedom. In fact, amongst the four scalar quantities that describe the perturbations in the metric and the two that describe the perturbations in the scalar fields, we can choose to work with any two of them to evolve the perturbations. The usual choices are the curvature and the isocurvature perturbations, which are actually a linear combination of the perturbations in the scalar fields [32–34]. In this section, we shall derive the equations governing the evolution of the perturbations in the two scalar fields, say, $\delta\phi$ and $\delta\chi$. Thereafter, we shall construct the curvature and isocurvature perturbations for our model and arrive at the equations describing them. As in our earlier model [26], we find that some of the coefficients in the equations governing the curvature and the isocurvature perturbations diverge as one approaches the bounce. To circumvent this difficulty, we shall choose two other independent scalar quantities to evolve the perturbations across the bounce and reconstruct the curvature and isocurvature perturbations from these quantities.

A. The Einstein's equations and the equations describing the perturbations in the scalar fields

In linear perturbation theory, the scalar and tensor perturbations evolve independently. When the scalar perturbations are taken into account, the FLRW line element, in general, can be written as

$$ds^2 = -(1 + 2A) dt^2 + 2a(t) (\partial_i B) dt dx^i + a^2(t) [(1 - 2\psi) \delta_{ij} + 2(\partial_i \partial_j E)] dx^i dx^j, \quad (23)$$

where A , B , ψ and E are four scalar functions that describe the perturbations, which depend on time as well as space. At the first order in the perturbations, the Einstein's equations describing the system of our interest are given by [1, 3–6]

$$3H \left(H A + \dot{\psi} \right) - \frac{1}{a^2} \nabla^2 \left[\psi - a H \left(B - a \dot{E} \right) \right] = -\frac{1}{2M_{\text{Pl}}^2} (\delta\rho_\phi + \delta\rho_\chi), \quad (24a)$$

$$\partial_i \left(H A + \dot{\psi} \right) = \frac{1}{2M_{\text{Pl}}^2} \partial_i (\delta q_\phi + \delta q_\chi), \quad (24b)$$

$$\ddot{\psi} + H \left(\dot{A} + 3\dot{\psi} \right) + \left(2\dot{H} + 3H^2 \right) A = \frac{1}{2M_{\text{Pl}}^2} (\delta p_\phi + \delta p_\chi), \quad (24c)$$

$$A - \psi + \frac{1}{a} \left[a^2 \left(B - a \dot{E} \right) \right]' = 0 \quad (24d)$$

where $\delta\rho_I$ and δp_I , with $I = (\phi, \chi)$, are the perturbations in the energy densities and pressure associated with the two fields ϕ and χ . Moreover, the quantities δq_I are related to the time-space components of the perturbed stress-energy

tensor through the condition $\delta T_{i(I)}^0 = -\partial_i(\delta q_I)$. The final equation arises due to the fact that the scalar fields do not possess any anisotropic stress. The components of the perturbed stress-energy tensor associated with the two fields ϕ and χ can be obtained to be

$$\delta T_{0(\phi)}^0 = -\delta\rho_\phi = -\dot{\phi}\delta\dot{\phi} + A\dot{\phi}^2 - V_\phi\delta\phi, \quad (25a)$$

$$\delta T_{i(\phi)}^0 = -\partial_i\delta q_\phi = -\partial_i(\dot{\phi}\delta\phi), \quad (25b)$$

$$\delta T_{j(\phi)}^i = \delta p_\phi\delta_j^i = \left(\dot{\phi}\delta\dot{\phi} - A\dot{\phi}^2 - V_\phi\delta\phi\right)\delta_j^i, \quad (25c)$$

and

$$\delta T_{0(\chi)}^0 = -\delta\rho_\chi = -(2b-1)bU_0(X^{xx})^{b-1}\dot{\chi}(\delta\dot{\chi} - \dot{\chi}A), \quad (26a)$$

$$\delta T_{i(\chi)}^0 = -\partial_i\delta q_\chi = bU_0(X^{xx})^{b-1}\dot{\chi}\delta\chi, \quad (26b)$$

$$\delta T_{j(\chi)}^i = \delta p_\chi\delta_j^i = \frac{\delta\rho_\chi}{2b-1}\delta_j^i, \quad (26c)$$

respectively.

A straightforward way to arrive at the equations of motion describing the perturbations in the scalar fields would be to utilize the conservation equation governing the perturbation in the stress-energy tensor of the fields. The equation describing the conservation of the perturbation in the energy density of a particular component is given by (see, for instance, Refs. [33, 34]):

$$\dot{\rho}_I + 3H(\delta\rho_I + \delta p_I) - 3(\rho_I + p_I)\dot{\psi} - \nabla^2\left[\left(\frac{\rho_I + p_I}{a}\right)B + \frac{\delta q_I}{a^2} - (\rho_I + p_I)\dot{E}\right] = 0. \quad (27)$$

On substituting the expressions for the components of the perturbed stress-energy tensor we have obtained in the above equation, we find that the equations of motion governing the Fourier modes, say, $\delta\phi_k$ and $\delta\chi_k$, associated with the perturbations in the two scalar fields can be expressed as

$$\ddot{\delta\phi}_k + 3H\dot{\delta\phi}_k + V_{\phi\phi}\delta\phi_k + 2V_\phi A_k - \dot{\phi}\left(\dot{A}_k + 3\dot{\psi}_k\right) + \frac{k^2}{a^2}\left[\delta\phi_k + a\dot{\phi}\left(B_k - a\dot{E}_k\right)\right] = 0, \quad (28a)$$

$$\ddot{\delta\chi}_k + \frac{3H}{2b-1}\dot{\delta\chi}_k - \dot{\chi}\left(\dot{A}_k + \frac{3\dot{\psi}_k}{2b-1}\right) + \frac{k^2}{(2b-1)a^2}\left[\delta\chi_k + a\dot{\chi}\left(B_k - a\dot{E}_k\right)\right] = 0. \quad (28b)$$

In these equations, the quantities A_k , B_k , ψ_k and E_k are the Fourier modes associated with the corresponding metric perturbations. Note that, when $b = 2$, these equations reduce to the matter bounce model we had considered in our earlier work [26].

In the following subsection, we shall first construct the gauge invariant curvature and isocurvature perturbations. Thereafter, with the aid of the above equations for $\delta\phi_k$ and $\delta\chi_k$, we shall arrive at the equations governing them. As in the case of the matter bounce scenario [26], we shall find that some of the coefficients in the equations governing the curvature and the isocurvature perturbations diverge in the domain where the null energy condition is violated around the bounce. Lastly, we shall discuss the method by which we can circumvent these difficulties before proceeding to solve the equations numerically.

B. Equations governing the scalar perturbations, and circumventing the diverging coefficients

Recall that the curvature perturbations are the fluctuations along the direction of the background trajectory in the field space. Whereas, the isocurvature perturbations correspond to fluctuations in a direction perpendicular to the background trajectory [32–34]. Using the arguments we had presented in our earlier work [26, 35], we can construct the curvature and the isocurvature perturbations for the model of our interest here to be

$$\mathcal{R} = \frac{H}{\dot{\phi}^2 - 2bU_0(X^{xx})^b}\left(\dot{\phi}\overline{\delta\phi} - bU_0(X^{xx})^{b-1}\dot{\chi}\overline{\delta\chi}\right), \quad (29a)$$

$$\mathcal{S} = \frac{H\sqrt{bU_0(X^{xx})^{b-1}}}{\dot{\phi}^2 - 2bU_0(X^{xx})^b}\left(\dot{\chi}\overline{\delta\phi} - \dot{\phi}\overline{\delta\chi}\right), \quad (29b)$$

where $\overline{\delta\phi} = \delta\phi + (\dot{\phi}/H)\psi$ and $\overline{\delta\chi} = \delta\chi + (\dot{\chi}/H)\psi$ are the gauge invariant versions of the perturbations associated with the two scalar fields. Upon using the equations of motion (28) governing the perturbations $\delta\phi_k$ and $\delta\chi_k$ and the first order Einstein's equations (24), we can arrive at the following equations governing the Fourier modes \mathcal{R}_k and \mathcal{S}_k of the curvature and the isocurvature perturbations:

$$\mathcal{R}_k'' + \left\{ \frac{2}{3(1+\lambda)[1-(3+2\lambda)k_0^2\eta^2]} \right\} [C_{rr}\mathcal{R}'_k + D_{rr}\mathcal{R}_k + C_{rs}\mathcal{S}'_k + D_{rs}\mathcal{S}_k] = 0, \quad (30a)$$

$$\mathcal{S}_k'' + \left\{ \frac{2}{3(1+\lambda)[1-(3+2\lambda)k_0^2\eta^2]} \right\} [C_{ss}\mathcal{S}'_k + D_{ss}\mathcal{S}_k + C_{sr}\mathcal{R}'_k + D_{sr}\mathcal{R}_k] = 0, \quad (30b)$$

where the quantities $(C_{rr}, D_{rr}, C_{rs}, D_{rs})$ are given by

$$C_{rr} = \frac{1}{(1-\lambda)(1+k_0^2\eta^2)\eta} \left[21 + 124\lambda + 219\lambda^2 + 144\lambda^3 + 32\lambda^4 \right. \\ \left. + (1+2\lambda)(27+76\lambda+61\lambda^2+16\lambda^3)k_0^2\eta^2 - 6(1+\lambda)^2(1-\lambda)(3+2\lambda)k_0^4\eta^4 \right], \quad (31a)$$

$$D_{rr} = -\frac{k^2}{2} \left[5 + 17\lambda + 8\lambda^2 + 3(1+\lambda)(3+2\lambda)k_0^2\eta^2 \right], \quad (31b)$$

$$C_{rs} = -\frac{\sqrt{2(2+\lambda)(3+2\lambda)}}{(1-\lambda)\sqrt{1+k_0^2\eta^2}\eta} \left[(1+2\lambda)(5+17\lambda+8\lambda^2) + 3(1+\lambda)(4+7\lambda+4\lambda^2)k_0^2\eta^2 \right], \quad (31c)$$

$$D_{rs} = \frac{\sqrt{2(2+\lambda)(3+2\lambda)}}{(1-\lambda)(1+k_0^2\eta^2)^{3/2}\eta^2} \left[(1+2\lambda)(5+17\lambda+8\lambda^2) + (1-\lambda)(1+2\lambda)(1+k_0^2\eta^2)^2 k^2\eta^2 \right. \\ \left. - 6(1+\lambda)(1+2\lambda)(4+7\lambda+4\lambda^2)k_0^4\eta^4 - (1+\lambda)(22+87\lambda+84\lambda^2+32\lambda^3)k_0^2\eta^2 \right], \quad (31d)$$

while the quantities $(C_{ss}, D_{sr}, C_{sr}, D_{ss})$ are given by

$$C_{ss} = -\frac{1}{(1-\lambda)(1+k_0^2\eta^2)\eta} \left[27 + 124\lambda + 213\lambda^2 + 144\lambda^3 + 32\lambda^4 \right. \\ \left. + (1+2\lambda)(21+76\lambda+67\lambda^2+16\lambda^3)k_0^2\eta^2 + 6(1+\lambda)^2(1-\lambda)(3+2\lambda)k_0^4\eta^4 \right], \quad (32a)$$

$$D_{ss} = \frac{1}{2(1-\lambda)(1+k_0^2\eta^2)^2\eta^2} \left\{ 2(27+124\lambda+213\lambda^2+144\lambda^3+32\lambda^4) \right. \\ - (255+1076\lambda+1753\lambda^2+1500\lambda^3+688\lambda^4+128\lambda^5)k_0^2\eta^2 \\ - (1+\lambda)(75+691\lambda+1314\lambda^2+936\lambda^3+224\lambda^4)k_0^4\eta^4 - 6(1-\lambda)(1+\lambda)(1+2\lambda)(3+2\lambda)k_0^6\eta^6 \\ \left. + (1-\lambda)[9+19\lambda+8\lambda^2-(1-\lambda)(3+2\lambda)k_0^2\eta^2](1+k_0^2\eta^2)^2 k^2\eta^2 \right\}, \quad (32b)$$

$$C_{sr} = \frac{\sqrt{2(2+\lambda)(3+2\lambda)}}{(1-\lambda)\sqrt{1+k_0^2\eta^2}\eta} \left[(1+2\lambda)(9+19\lambda+8\lambda^2) - (1-\lambda)(2+\lambda)(3+4\lambda)k_0^2\eta^2 \right], \quad (32c)$$

$$D_{sr} = -\sqrt{2(2+\lambda)(3+2\lambda)}(1+2\lambda)k^2\sqrt{1+k_0^2\eta^2}. \quad (32d)$$

We find that some of these coefficients diverge either at the time when $\dot{H} = 0$ or at the bounce. This poses a difficulty in evolving the curvature and the isocurvature perturbations across these instances. As we had done in our earlier work [26], around the bounce, we shall work in a specific gauge wherein the two scalar quantities describing the perturbations behave well at such points. We shall evolve these two scalar quantities across these domains and eventually reconstruct the curvature and the isocurvature perturbations from these quantities. Note that $\dot{H} = 0$ when $\eta_* = \mp 1/[\sqrt{(3+2\lambda)k_0}]$. As we shall illustrate later, the curvature and the isocurvature perturbations indeed diverge at this point (in this context, see our discussion in App. A). Also, we shall find that, while the isocurvature perturbations vanish exactly at the bounce, the curvature perturbations go to zero a little time later.

As we had mentioned, we shall overcome the problem of diverging coefficients by working in a specific gauge. It has been observed that the difficulties of evolving the curvature and the isocurvature perturbations across the bounce can be avoided if we choose to work in the uniform- χ gauge, *i.e.* the gauge wherein $\delta\chi_k = 0$ [26, 27]. In this gauge,

we can use A and ψ as the two independent scalar functions and these quantities can be smoothly evolved across the bounce. The curvature and the isocurvature perturbations can then be suitably constructed from these two scalar perturbations. In uniform χ -gauge, Eq. (28b) reduces to

$$\frac{k^2}{a} \left(B_k - a \dot{E}_k \right) = (2b - 1) \dot{A}_k + 3 \dot{\psi}_k. \quad (33)$$

Upon using this relation, the first order Einstein equations (24) and the background equations, we obtain the following equations governing A_k and ψ_k :

$$A_k'' + \frac{4(2+3\lambda)k_0^2\eta}{1+k_0^2\eta^2} A_k' + \frac{k^2(1+k_0^2\eta^2)^2(1-\lambda) - 12k_0^2(1+\lambda)^2(5+4\lambda)}{3(1+\lambda)(1+k_0^2\eta^2)^2} A_k = -\frac{2(1-\lambda)(3+4\lambda)k_0^2\eta}{(1+\lambda)(1+k_0^2\eta^2)} \psi_k' + \frac{4(1-\lambda)}{3(1+\lambda)} k^2 \psi_k, \quad (34a)$$

$$\psi_k'' - \frac{2(1+2\lambda)k_0^2\eta}{1+k_0^2\eta^2} \psi_k' + k^2 \psi_k = \frac{4(1+\lambda)(1+2\lambda)k_0^2\eta}{(1-\lambda)(1+k_0^2\eta^2)} A_k' - \frac{4(1+\lambda)^2(5+4\lambda)}{(1-\lambda)(1+k_0^2\eta^2)^2} k_0^2 A_k. \quad (34b)$$

Note that, in the uniform χ -gauge, the curvature and the isocurvature perturbations are given by

$$\mathcal{R}_k = \psi_k + \frac{2HM_{\text{Pl}}^2}{\dot{\phi}^2 - 2bU_0(X^{\text{xx}})^b} \left(\dot{\psi}_k + H A_k \right), \quad (35a)$$

$$\mathcal{S}_k = \frac{2HM_{\text{Pl}}^2 \sqrt{bU_0(X^{\text{xx}})^{b-1}} \dot{\chi}}{\left[\dot{\phi}^2 - 2bU_0(X^{\text{xx}})^b \right] \dot{\phi}} \left(\dot{\psi}_k + H A_k \right). \quad (35b)$$

Later, we shall make use of these relations to construct \mathcal{R}_k and \mathcal{S}_k from A_k and ψ_k around the bounce.

V. EVOLUTION OF THE PERTURBATIONS AND POWER SPECTRA

In our earlier work on the matter bounce scenario [26], we had constructed analytical as well as numerical solutions for the perturbations at early times (*i.e.* when $\eta \ll -\eta_0$) as well across the bounce. For the case of near-matter bounces of our interest here, we do not seem to be able to analytically solve the equations (34) governing A_k and ψ_k across the bounce. Therefore, we evolve the perturbations numerically. In the case of bounces driven by two fields, one of the concerns that has been raised is whether the fields will be decoupled at early times allowing one to impose the required Bunch-Davies initial conditions (in this context, see Ref. [36]). Note that, in the model governed by the action (4), the two fields ϕ and χ do not interact directly and are coupled only gravitationally. It should be clear from the first Friedmann equation (3) that the energy densities of the two fields are equal *only at the bounce*. Clearly, at very early times, the background universe is effectively driven by a single field, with the field ϕ dominating the evolution. This behavior ensures that the curvature and the iso-curvature perturbations are completely decoupled during the early contracting phase permitting us to impose the standard initial conditions on the modes.

As we can construct the background quantities analytically, we shall require the numerical procedure only for the evolution of the perturbations. The tensor perturbations can be evolved across the bounce without any diffi-

culty. In the case of scalars, we evolve the curvature and the isocurvature perturbations until close to the bounce and thereafter we shall choose to evolve the metric perturbations A_k and ψ_k across the bounce (for reasons discussed in the last section). We shall evaluate the final perturbation spectra at a suitable time after the bounce.

A. Analytical solutions at early times

Since the scale factor (2) reduces to a power law form for $\eta \ll -\eta_0$, the scalar modes can be obtained analytically during the contracting phase as in the case of tensors. Also, as we mentioned, during these early times, it is the energy density of the scalar field ϕ that dominates the background evolution. Due to this reason, as we discussed, when $\eta \ll -\eta_0$, the curvature and the isocurvature perturbations decouple so that the equations (30) governing \mathcal{R}_k and \mathcal{S}_k simplify to

$$\mathcal{R}_k'' + 2 \frac{z'}{z} \mathcal{R}_k' + k^2 \mathcal{R}_k \simeq 0, \quad (36a)$$

$$\mathcal{S}_k'' + 2 \frac{z'}{z} \mathcal{S}_k' + \left[w_\chi k^2 + \frac{2(1+2\lambda)}{\eta^2} \right] \mathcal{S}_k \simeq 0, \quad (36b)$$

where $z \simeq a \dot{\phi}/H \simeq \sqrt{3(1+w_\phi)} M_{\text{Pl}} a$ and, recall that, while $w_\phi = -\lambda/[3(1+\lambda)]$, $w_\chi = (1-\lambda)/[3(1+\lambda)]$. We find that the equations describing the Mukhanov-Sasaki variables corresponding to the curvature and the isocurvature perturbations, *viz.* $\mathcal{U}_k = z \mathcal{R}_k$ and $\mathcal{V}_k =$

$z\mathcal{S}_k$, reduce to

$$\mathcal{U}_k'' + \left[k^2 - \frac{2(1+\lambda)(1+2\lambda)}{\eta^2} \right] \mathcal{U}_k \simeq 0, \quad (37a)$$

$$\mathcal{V}_k'' + \left[w_\chi k^2 - \frac{2\lambda(1+2\lambda)}{\eta^2} \right] \mathcal{V}_k \simeq 0. \quad (37b)$$

At very early times during the contracting phase, *i.e.* when $\eta \ll -\eta_0$, we can impose the following Bunch-Davies initial conditions on the scalar Mukhanov-Sasaki variables \mathcal{U}_k and \mathcal{V}_k :

$$\mathcal{U}_k(\eta) = \frac{1}{\sqrt{2k}} e^{-ik\eta}, \quad (38a)$$

$$\mathcal{V}_k(\eta) = \frac{1}{\sqrt{2w_\chi^{\frac{1}{2}}k}} e^{-i\sqrt{w_\chi}k\eta}. \quad (38b)$$

For convenience, let us simply define the scalar power spectra to be (in this context, see the following subsection where we discuss the numerical evolution of the perturbations)

$$\mathcal{P}_\mathcal{R}(k) = \frac{k^3}{2\pi^2} |\mathcal{R}_k|^2, \quad (39a)$$

$$\mathcal{P}_\mathcal{S}(k) = \frac{k^3}{2\pi^2} |\mathcal{S}_k|^2. \quad (39b)$$

The spectral index $n_\mathcal{R}$ of the curvature perturbation is given by

$$n_\mathcal{R} = 1 + \frac{d \ln \mathcal{P}_\mathcal{R}}{d \ln k}. \quad (40)$$

Note that the equation governing the tensor and scalar Mukhanov-Sasaki variables u_k and \mathcal{U}_k [cf. Eqs. (19) and (37a)] at early times during the contracting phase have the same form, as is expected in a power law background. Therefore, the spectrum of curvature perturbations evaluated prior to the bounce has the same shape as the tensor power spectrum. As a result, we find that, we can write

$$\mathcal{P}_\mathcal{T}(k) = r \mathcal{P}_\mathcal{R}(k), \quad (41)$$

where the tensor-to-scalar ratio r is a constant and is given by

$$r = \frac{8(3+2\lambda)}{1+\lambda}. \quad (42)$$

Evidently, $r = 24$ when $\lambda = 0$, a well known result in the matter bounce scenarios (see, for instance, Ref. [27]). It should also be mentioned that the spectral index $n_\mathcal{R}$ is given by

$$n_\mathcal{R} = 1 - 4\lambda. \quad (43)$$

B. Numerical evolution across the bounce

We evolve the perturbations numerically just as we had done in our earlier work [26]. To begin with, we use

e-N-folds \mathcal{N} —defined as $a(\mathcal{N}) = a_0 \exp(\mathcal{N}^2/2)$ —to be our independent variable. The e-N-fold proves to be very convenient to describe symmetric bounces and it replaces the more conventional e-fold to evolve the perturbations over a wide domain in time efficiently [26, 28, 29]. We express the equations (15) and (30) governing the tensor and scalar perturbations h_k , \mathcal{R}_k and \mathcal{S}_k in terms of the new variable \mathcal{N} and integrate the equations using a fifth order Runge-Kutta algorithm. In the case of the scalar perturbations, as is often done in the case of two field models, we shall numerically integrate the equations (30) using two sets of initial conditions (in this context, see, for instance, Refs. [35, 37]). We first integrate the equations by imposing the Bunch-Davies initial condition corresponding to (38a) on \mathcal{R}_k and setting the initial value of \mathcal{S}_k to be zero. We then impose the initial condition corresponding to (38b) on \mathcal{S}_k and set the initial value of \mathcal{R}_k to be zero. If the perturbations \mathcal{R}_k and \mathcal{S}_k evolved according to these two sets of initial conditions are denoted as $(\mathcal{R}_k^I, \mathcal{S}_k^I)$ and $(\mathcal{R}_k^{II}, \mathcal{S}_k^{II})$, then the power spectra associated with the curvature and the isocurvature perturbations can be defined as [35, 37]

$$\mathcal{P}_\mathcal{R}(k) = \frac{k^3}{2\pi^2} \left(|\mathcal{R}_k^I|^2 + |\mathcal{R}_k^{II}|^2 \right), \quad (44a)$$

$$\mathcal{P}_\mathcal{S}(k) = \frac{k^3}{2\pi^2} \left(|\mathcal{S}_k^I|^2 + |\mathcal{S}_k^{II}|^2 \right). \quad (44b)$$

We had discussed earlier as to how the model of our interest depends only on two parameters, *viz.* k_0/a_0 and λ . If we multiply the modes \mathcal{R}_k , \mathcal{S}_k and h_k by the quantity $\sqrt{k_0} a_0 M_{\text{Pl}}$, we find that k_0 or a_0 need not be specified independently in order to evolve them from the given initial conditions. In fact, the resulting scalar and tensor power spectra depend only on k_0/a_0 and λ . We shall choose to work with $k_0/(a_0 M_{\text{Pl}}) = 9.61 \times 10^{-9}$ and $\lambda = 0.01$. This value of k_0/a_0 ensures that the curvature perturbation spectrum $\mathcal{P}_\mathcal{R}(k)$ evaluated after the bounce is COBE normalized corresponding to the value of 2.31×10^{-9} at a suitable pivot scale. Also, the value of λ we shall work with leads to the scalar spectral index of $n_\mathcal{R} \simeq 0.96$, as required by the Planck data.

We impose the initial conditions on the perturbations when $k^2 = 10^4 (a''/a)$. In the case of tensors, we evolve the equation (15) across the bounce (with \mathcal{N} as the independent variable) until $\eta = \beta \eta_0$, with $\beta = 10^2$, after the bounce. We evolve the scalar perturbations using the equations (30) until $\eta = -\alpha \eta_0$ and we shall assume that $\alpha = 10^5$. Since the equations (30) contain coefficients which diverge close to the bounce, as we had discussed, we instead use equations (34) to evolve the scalar perturbations A_k and ψ_k across the bounce from $\eta = -\alpha \eta_0$ to $\eta = \beta \eta_0$. Evidently, the quantities \mathcal{R}_k and \mathcal{S}_k evolved during the early contracting phase can provide us the initial conditions for A_k and ψ_k at $\eta = -\alpha \eta_0$ through the relations (35). Once we have A_k and ψ_k in hand, we shall reconstruct \mathcal{R}_k and \mathcal{S}_k using the same relations. It is useful to mention here that, for the values of k_0/a_0 and λ that we are working with, $\eta = -\alpha \eta_0$ with $\alpha = 10^5$

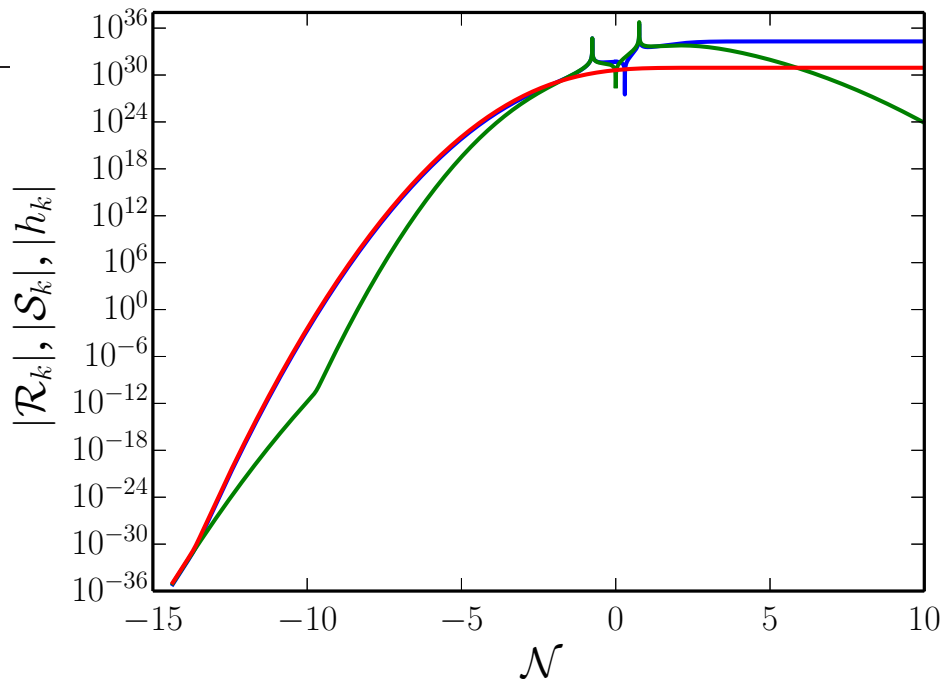


FIG. 1. Evolution of the amplitudes of the curvature perturbation \mathcal{R}_k (in blue), the isocurvature perturbation \mathcal{S}_k (in green) and the tensor mode h_k (in red) corresponding to the wavenumber $k/k_0 = 10^{-20}$ has been plotted as a function of e-N-folds \mathcal{N} . We have chosen the background parameters to be $k_0/(a_0 M_{\text{Pl}}) = 9.6 \times 10^{-9}$ and $\lambda = 0.01$ in plotting this figure. We should clarify that we have, in fact, multiplied \mathcal{R}_k , \mathcal{S}_k and h_k by the quantity $\sqrt{k_0} a_0 M_{\text{Pl}}$ to ensure that they depend only on the parameters k_0/a_0 and λ . We have plotted the numerical results from the initial e-N-fold when $k^2 = 10^4 (a''/a)$ corresponding to the mode. The behavior of the modes is essentially similar to their behavior in the matter bounce scenario we had considered in our earlier work [26]. The sharp rise in the amplitude of the curvature perturbation close to the bounce ensures that the tensor-to-scalar ratio is strongly suppressed after the bounce leading to levels of r that are consistent with the upper bounds from Planck. Moreover, note that the isocurvature perturbation decays after the bounce, which leads to a strongly adiabatic spectrum, as is also required by the observations.

corresponds to $\mathcal{N} \simeq -6.78$, while $\eta = \beta \eta_0$ with $\beta = 10^2$ corresponds to $\mathcal{N} = 4.29$.

C. Behavior of the perturbations and the power spectra

In Fig. 1, we have plotted the evolution of the perturbations \mathcal{R}_k and \mathcal{S}_k and h_k for a typical cosmological scale as a function of e-N-folds \mathcal{N} . As we had expected, the curvature and the isocurvature perturbations diverge at the points where $\dot{H} = 0$, *i.e.* at $\eta_*^\mp = \mp 1/[\sqrt{(3+2\lambda)} k_0]$, corresponding to $\mathcal{N} = \mp 0.76$ (in this context, see App. A). Moreover, as expected, the isocurvature perturbations vanish at the bounce. We find that, in fact, the curvature perturbation also vanishes at a point soon after the bounce. Further, while the amplitude of the curvature and the tensor perturbations freeze after $\eta = \eta_*^+$, the isocurvature perturbations decay soon after². Such a decay leads to a strongly adiabatic spectrum of scalar perturbations, as is required by the observations. All these points should be evident from Fig. 1. Essentially, the scalar and tensor perturbations behave just as in the matter bounce scenario we had considered earlier [26].

Having obtained the solutions for the modes, we can now evaluate the resulting power spectra. We compute the scalar and tensor power spectra after the bounce at $\eta = \beta \eta_0$, with $\beta = 10^2$ (corresponding to $\mathcal{N} = 4.29$). In

² In fact, in the case of the tensor perturbations, it is possible to construct analytical solutions across the bounce as well (in this

context, see Ref. [38]). We find that our numerical solutions match the analytical solutions quite well.

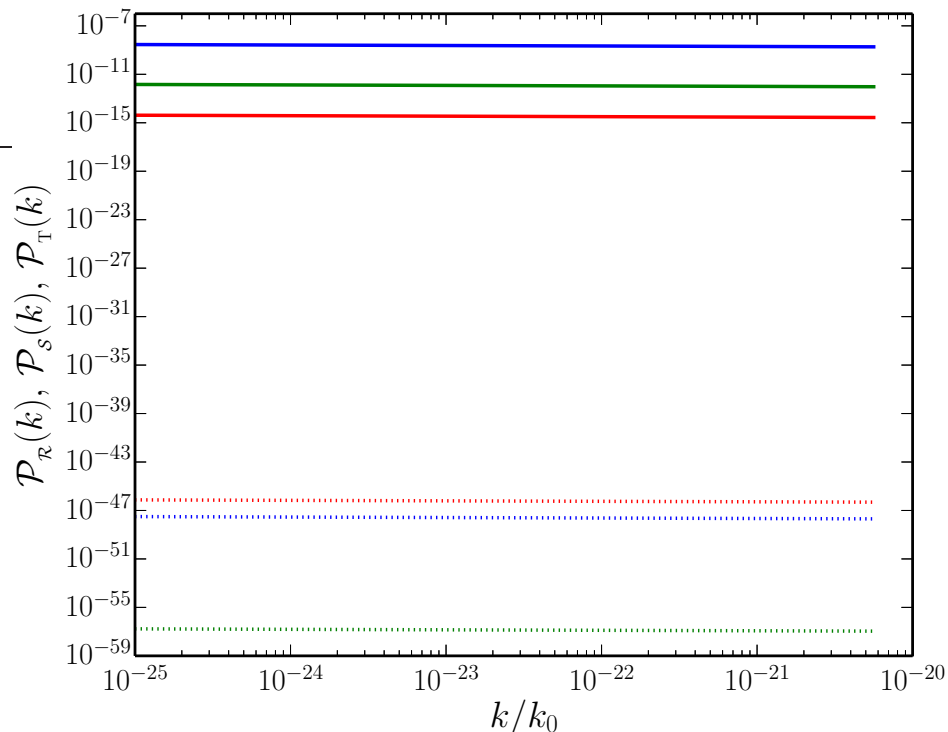


FIG. 2. The numerically evaluated scalar (the curvature perturbation spectrum in blue and the isocurvature perturbation spectrum in green) and tensor power spectra (in red) have been plotted as a function of k/k_0 for a range of wavenumbers that correspond to cosmological scales today. We have worked with the same set of values for the parameters k_0/a_0 and λ as in the previous figure. The power spectra have been plotted both before the bounce (as dotted lines) and after (as solid lines). The power spectra have been evaluated at $\eta = -\alpha\eta_0$ (with $\alpha = 10^5$) before the bounce and at $\eta = \beta\eta_0$ (with $\beta = 10^2$) after the bounce. The values for the parameters we have worked with lead to the COBE normalized value of 2.31×10^{-9} for the curvature perturbation spectrum at the scale of $k/k_0 = 10^{-23}$. Also, the value of λ we have chosen leads to a curvature perturbation spectrum with a red tilt corresponding to $n_{\mathcal{R}} \simeq 0.96$, as required by the CMB observations. Moreover, the tensor-to-scalar ratio evaluated after the bounce proves to be rather small ($r \simeq 10^{-6}$), which is consistent with the current upper limits from Planck on the quantity [10].

Fig. 2, we have plotted the power spectra prior to the bounce (evaluated at $\eta = -\alpha\eta_0$, with $\alpha = 10^5$, corresponding to $\mathcal{N} = -6.78$) as well as after the bounce. It is evident from the figure that the shape of the power spectra are preserved as the perturbations evolve across the bounce. We find that the value of $k_0/(a_0 M_{\text{Pl}}) = 9.61 \times 10^{-9}$ leads to the COBE normalized value of 2.31×10^{-9} for the curvature perturbation spectrum at the scale of $k/k_0 = 10^{-23}$. Recall that, our main goal here is introduce a suitable tilt to the curvature perturbation spectrum so as to be consistent with the observations. As we had mentioned, for $\lambda = 0.01$, we find that $n_{\mathcal{R}} = 0.96$, perfectly consistent with the observations. Lastly, we find that, as the perturbations evolve across the bounce, the tensor-to-scalar ratio drops from the value of $r = 23.92$ prior to the bounce to $r = 1.46 \times 10^{-6}$ after the bounce. Needless to add, this value of the r is much smaller than the current upper bound of $r \lesssim 0.07$ from Planck [10].

VI. DISCUSSION

In this work, extending our earlier effort, we have constructed a two field model consisting of a canonical scalar field and a non-canonical ghost field to drive near-matter bounces. Near-matter bounces are in some sense similar to slow roll inflation as they lead to nearly scale invariant spectra. The model we have constructed consisted of two parameters k_0/a_0 and λ . While k_0/a_0 determines

the amplitudes of the scalar and tensor power spectra, a non-zero value for λ leads to a tilt in the power spectra. We have been able to numerically evaluate the scalar and tensor power spectra in the model and show that, for suitable values of the parameters, the resulting spectra are consistent with the current constraints from the CMB observations.

It is interesting to have extended our original matter bounce scenario and have achieved a red tilt in the scalar power spectrum in order to be consistent with the ob-

servations. The next obvious challenge is to examine if the scalar non-Gaussianities generated in the model are indeed consistent with the current constraints from Planck [11]. We are presently investigating this issue.

ACKNOWLEDGEMENTS

LS wishes to thank the Indian Institute of Technology Madras, Chennai, India, for support through the Exploratory Research Project PHY/17-18/874/RFER/LSRI.

Appendix A: Is a diverging curvature perturbation acceptable?

We have seen that, in the model driving near-matter bounces we have constructed here as well as the earlier model leading to the matter bounce scenario [26], the curvature and the isocurvature perturbations diverge when $\dot{H} = 0$. This may cause concern as to whether the perturbation theory breaks down around such instances. We believe that this behavior should not be of any concern. The reason being that the curvature and the isocurvature perturbations diverge due to the fact that a background quantity that appears in the denominator of their definitions vanish. As we have discussed, it is possible to overcome such hurdles by working with perturbed quantities that behave well at these points.

In fact, such a behavior also occurs during the reheating phase that succeeds inflation. To illustrate this point, let us consider the often studied case of inflation driven by a single, canonical scalar field, say, φ . As is well known, once inflation has terminated, the scalar field is expected to oscillate at the bottom of the potential between the turning points where the velocity of the field vanishes. Let us focus on the domain where the energy density of the scalar field is still dominant soon after inflation (*i.e.* when reheating is yet to set in, a period that is referred to as preheating). In such a situation, for the case of inflation and preheating driven by the conventional quadratic potential, the behavior of the background as well as the curvature perturbation associated with a typical large scale mode of cosmological interest can be solved for analytically (in this context, see, for instance, Ref. [39]). In Fig. A, we have plotted the evolution of the velocity $\dot{\varphi}$ of the background scalar field and the curvature perturbation, say, \mathcal{R}_k , associated with a small scale mode obtained numerically, as a function of e-fold N during the epoch of preheating. In plotting the figure, for convenience, we have chosen to work with a small range of e-folds of inflation. Also, we have restricted ourselves to the behavior of the velocity of the scalar field and the curvature perturbation during the epoch of preheating. It is clear from the figure that the curvature perturbation diverges exactly at the turning points when the scalar field oscillates at the bottom of

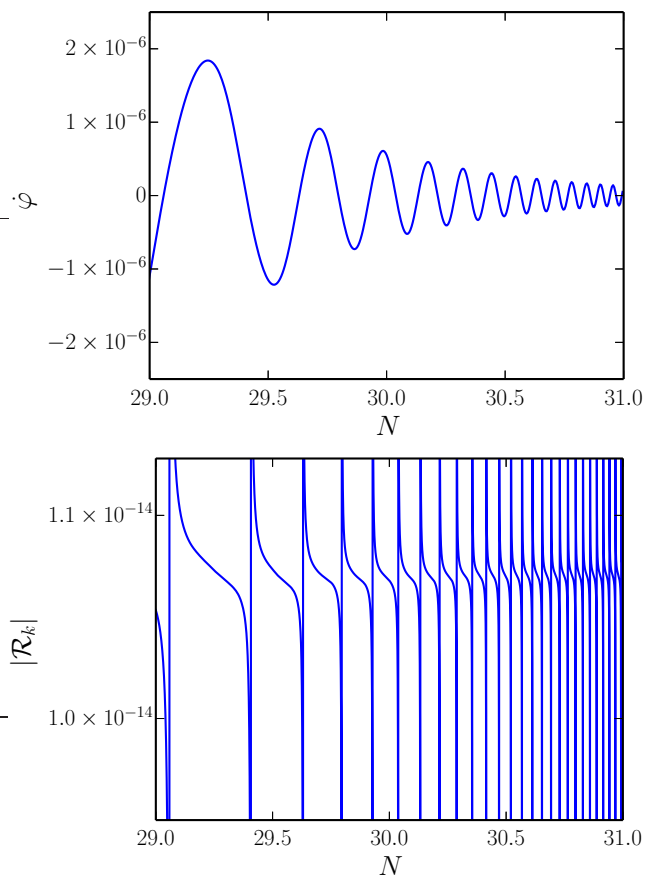


FIG. 3. The behavior of the velocity $\dot{\varphi}$ of the scalar field driving the background (on top) and the amplitude of the curvature perturbation \mathcal{R}_k (at the bottom), obtained numerically, have been plotted as a function of e-fold N during the epoch of preheating that succeeds inflation. For purposes of illustration, we have considered the simple case of the conventional quadratic potential to drive inflation and preheating. Also, for convenience, we have chosen to work with a small period of inflation and have highlighted the behavior of the velocity of the field and the amplitude of the curvature perturbation during the epoch of preheating (in this context, also see Ref. [39]). For our choice of the parameters and initial conditions, inflation ends at $N \simeq 28.3$ and the mode of interest leaves the Hubble scale during inflation at $N \simeq 26.2$. It is evident from the figures that the curvature perturbation diverges *exactly* at the points where $\dot{\varphi}$ and, hence, \dot{H} vanish.

the inflationary potential. The situation encountered in the cases of the bouncing scenarios we have considered here is exactly similar to the behavior during preheating. In fact, in both the situations, the divergences occur whenever $\dot{H} = 0$. Due to this reason, we believe that the divergent curvature and isocurvature perturbations which we encounter in the bouncing models of our interest pose no cause for concern (for a discussion on this issue, also see Ref. [40]). There are two points which we wish to stress before we conclude. Note that the background is well behaved (say, no divergences in the cur-

vature invariants arise) at the points where \dot{H} vanishes. Moreover, we should clarify that we have made no ef-

fort to regularize the perturbations. We have chosen to work in suitably convenient gauges in order to evolve the perturbations across the points where \dot{H} vanishes.

-
- [1] V. F. Mukhanov, H. A. Feldman, and R. H. Brandenberger, *Phys. Rept.* **215**, 203 (1992).
- [2] J. Martin, *Particles and fields. Proceedings, 24th National Meeting, ENFPC 24, Caxambu, Brazil, September 30-October 4, 2003*, *Braz. J. Phys.* **34**, 1307 (2004), [arXiv:astro-ph/0312492](#) [astro-ph].
- [3] J. Martin, *Planck scale effects in astrophysics and cosmology. Proceedings, 40th Karpacs Winter School, Ladek Zdroj, Poland, February 4-14, 2004*, *Lect. Notes Phys.* **669**, 199 (2005), [arXiv:hep-th/0406011](#) [hep-th].
- [4] B. A. Bassett, S. Tsujikawa, and D. Wands, *Rev. Mod. Phys.* **78**, 537 (2006).
- [5] L. Sriramkumar, (2009), [arXiv:0904.4584](#) [astro-ph.CO].
- [6] L. Sriramkumar, in *Vignettes in Gravitation and Cosmology*, edited by L. Sriramkumar and T. Seshadri (World Scientific, Singapore, 2012) pp. 207–249.
- [7] D. Baumann, in *Physics of the large and the small, TASI 09, proceedings of the Theoretical Advanced Study Institute in Elementary P* (2011) pp. 523–686, [arXiv:0907.5424](#) [hep-th].
- [8] A. Linde, in *Proceedings, 100th Les Houches Summer School: Post-Planck Cosmology: Les Houches, France, July 8 - August 2, 2013* (2015) pp. 231–316, [arXiv:1402.0526](#) [hep-th].
- [9] J. Martin, *The Cosmic Microwave Background*, *Astrophys. Space Sci. Proc.* **45**, 41 (2016), [arXiv:1502.05733](#) [astro-ph.CO].
- [10] P. A. R. Ade *et al.* (Planck), (2015), [arXiv:1502.02114](#) [astro-ph.CO].
- [11] P. A. R. Ade *et al.* (Planck), (2015), [arXiv:1502.01592](#) [astro-ph.CO].
- [12] J. Martin, C. Ringeval, and R. Trotta, *Phys. Rev.* **D83**, 063524 (2011), [arXiv:1009.4157](#) [astro-ph.CO].
- [13] J. Martin, C. Ringeval, and V. Vennin, *Phys. Dark Univ.* **5-6**, 75235 (2014), [arXiv:1303.3787](#) [astro-ph.CO].
- [14] J. Martin, C. Ringeval, R. Trotta, and V. Vennin, *JCAP* **1403**, 039, [arXiv:1312.3529](#) [astro-ph.CO].
- [15] J. Martin, C. Ringeval, and V. Vennin, *JCAP* **1410** (10), 038, [arXiv:1407.4034](#) [astro-ph.CO].
- [16] G. Gubitosi, M. Lagos, J. Magueijo, and R. Allison, *JCAP* **1606** (06), 002, [arXiv:1506.09143](#) [astro-ph.CO].
- [17] M. Novello and S. P. Bergliaffa, *Phys. Rept.* **463**, 127 (2008), [arXiv:0802.1634](#) [astro-ph].
- [18] D. A. Easson, I. Sawicki, and A. Vikman, *JCAP* **1111**, 021, [arXiv:1109.1047](#) [hep-th].
- [19] Y.-F. Cai, *Sci. China Phys. Mech. Astron.* **57**, 1414 (2014), [arXiv:1405.1369](#) [hep-th].
- [20] D. Battfeld and P. Peter, *Phys. Rept.* **571**, 1 (2015), [arXiv:1406.2790](#) [astro-ph.CO].
- [21] M. Lilley and P. Peter, *Comptes Rendus Physique* **16**, 1038 (2015), [arXiv:1503.06578](#) [astro-ph.CO].
- [22] A. Ijjas and P. J. Steinhardt, *Class. Quant. Grav.* **33**, 044001 (2016), [arXiv:1512.09010](#) [astro-ph.CO].
- [23] R. Brandenberger and P. Peter, (2016), [arXiv:1603.05834](#) [hep-th].
- [24] D. Wands, *Phys. Rev.* **D60**, 023507 (1999), [arXiv:gr-qc/9809062](#) [gr-qc].
- [25] D. Wands, *Adv. Sci. Lett.* **2**, 194 (2009), [arXiv:0809.4556](#) [astro-ph].
- [26] R. N. Raveendran, D. Chowdhury, and L. Sriramkumar, *JCAP* **1801** (01), 030, [arXiv:1703.10061](#) [gr-qc].
- [27] L. E. Allen and D. Wands, *Phys. Rev.* **D70**, 063515 (2004), [arXiv:astro-ph/0404441](#) [astro-ph].
- [28] L. Sriramkumar, K. Atmjeet, and R. K. Jain, *JCAP* **09**, 010, [arXiv:1504.06853](#) [astro-ph.CO].
- [29] D. Chowdhury, V. Sreenath, and L. Sriramkumar, *JCAP* **1511**, 002, [arXiv:1506.06475](#) [astro-ph.CO].
- [30] J.-c. Hwang and H. Noh, *Phys. Rev.* **D65**, 124010 (2002), [arXiv:astro-ph/0112079](#) [astro-ph].
- [31] J. M. Maldacena, *JHEP* **05**, 013, [arXiv:astro-ph/0210603](#) [astro-ph].
- [32] C. Gordon, D. Wands, B. A. Bassett, and R. Maartens, *Phys. Rev.* **D63**, 023506 (2001), [arXiv:astro-ph/0009131](#) [astro-ph].
- [33] K. A. Malik and D. Wands, *JCAP* **0502**, 007, [arXiv:astro-ph/0411703](#) [astro-ph].
- [34] K. A. Malik and D. Wands, *Phys. Rept.* **475**, 1 (2009), [arXiv:0809.4944](#) [astro-ph].
- [35] Z. Lalak, D. Langlois, S. Pokorski, and K. Turzynski, *JCAP* **0707**, 014, [arXiv:0704.0212](#) [hep-th].
- [36] P. Peter, N. Pinto-Neto, and S. D. P. Vitiello, *Phys. Rev.* **D93**, 023520 (2016), [arXiv:1510.06628](#) [gr-qc].
- [37] S. Tsujikawa, D. Parkinson, and B. A. Bassett, *Phys. Rev.* **D67**, 083516 (2003), [arXiv:astro-ph/0210322](#) [astro-ph].
- [38] D. J. Stargen, V. Sreenath, and L. Sriramkumar, (2016), [arXiv:1605.07311](#) [gr-qc].
- [39] D. K. Hazra, J. Martin, and L. Sriramkumar, *Phys. Rev.* **D86**, 063523 (2012), [arXiv:1206.0442](#) [astro-ph.CO].
- [40] A. Ijjas, *JCAP* **1802** (02), 007, [arXiv:1710.05990](#) [gr-qc].